Bending of Sandwich Beams with Transversely Flexible Core

Y. Frostig* and M. Baruch†
Technion—Israel Institute of Technology, Haifa, Israel

The bending behavior of a sandwich beam with a foam core is analytically investigated. The beam consists of upper and lower skins, metallic or composite laminated, and a soft core. The loading pattern consists of concentrated as well as distributed loads exerted at the upper or the lower skin or a combination of the two. The analysis includes the effects of the flexibility of the core in the vertical direction on the overall bending behavior. The main parameters affecting the overall behavior and particularly the peeling and the shear stresses between the skins and the core are studied.

Introduction

SANDWICH beams have been used in various industries for many years. A typical beam consists of two skins made of metal or laminated composite and a core. The core is usually made of honeycomb, metallic or nonmetallic, which is stiff in the vertical direction and flexible in the horizontal one. In recent years, plastic foams are used for cores in sandwich structures. In this case, the effect of the transverse flexibility of the core on the mechanical behavior of the beam should be taken into account. This flexibility affects the transverse bending behavior of the beam and leads to unequal deflections of the upper and lower symmetrical skins (see Fig. 1).

Sandwich beams with honeycomb cores were considered by many researchers. Reissner[1,2] included the shear strain effect on the bending, but only the average bending behavior of the composite beam is considered. Many researchers[3-5] dealt with the analysis of beams with an antiplane core, i.e., a core with shear rigidity only. The Hexcel designer manual[6] outlines the design procedures for beams with honeycomb cores only. An antiplane-core approach with anisotropic and composite skin appears in Refs. 7-9. Ojalvo[10] assumed different deflections to the two skins, but neglected the peeling stresses. Ogorkiewicz and Sayigh[11] dealt with a foam core by replacing it with an ordinary beam with equivalent properties.

In this paper, the proposed analysis includes the effects of the transverse flexibility of the core and the peeling stresses between the skin face and the core on the overall bending behavior.

The analysis is general and applicable to metallic or composite laminated identical skins. The behavior is described in terms of the deflections, the peeling, and the shear stresses in the adhesive layers. The effect of the variables that govern the behavior is incorporated through a parametric study.

The mathematical formulation and the boundary conditions are discussed. The analytical solution for the various types of loading with different boundary conditions is presented.

Mathematical Formulation

The analysis is carried out by superposition of two types of beam behavior (see Fig. 2). The first one, substructure I, with an antiplane core (see Ref. 5) is loaded by two equal forces in the same direction, $q_t^{\mathrm{I}} = q_b^{\mathrm{I}} = (q_t + q_b)/2$. The second one, substructure II, in which the core height can be changed, is loaded by two equal forces $q_t^{\mathrm{II}} = q_b^{\mathrm{II}} = (q_t - q_b)/2$, which are self-equilibrated.

The assumptions used in deriving the governing equations include 1) skin deformation following classical beam theory—plane section remains plane and cross section deform normally to their individual middle surfaces; 2) the core has negligible normal stress rigidity in the horizontal directions, but can resist shear stresses and transverse normal stresses; 3) the adhesive layer between the skins and the core carries shear and transverse normal stresses; 4) elastic behavior; 5) the elastic shear strain in the skins is negligible; 6) deflections and rotations are small; and 7) load is applied at the skins only and the distance between the centroids of the skins is constant.

The governing equations are presented, their solutions are discussed, and the appropriate boundary conditions are given later.

Substructure I

The substructure consists of two identical skins and a core capable of resisting shear and transverse normal stresses. The upper and the lower skins are loaded by two equal loads acting in the same direction. Since the skins are subjected to the same loadings, the shear and the transverse normal stresses at the interfaces of the two skins and the core are identical.

The equilibrium equations derived by inspection of a differential segment are (see Fig. 4)

Upper skin (plate 1):

$$F_{1,x} = -\tau b \tag{1a}$$

$$Q_{1,x} = -q^{\mathrm{I}} + p^{\mathrm{I}}/2b \tag{1b}$$

$$M_{1,x} = Q_1 - \tau bd/2 \tag{1c}$$

Lower skin (plate 2):

$$F_{2,x} = -\tau b \tag{2a}$$

$$Q_{2,x} = -q^{\mathrm{I}} + p^{\mathrm{I}}/2b \tag{2b}$$

$$M_{2,x} = Q_2 - \tau bd/2 \tag{2c}$$

Core:

$$Q_{c,x} = -p^{\mathrm{I}} b \tag{3}$$

where b is the width of the beam; Q_i, F_i, M_i ($i = 1,2$) are the shear, axial forces, and bending moments, respectively, for the upper and the lower skins; and p^{I} and τ the transverse normal stresses and shear stresses, respectively.

Presented as Paper 88-2291 at the AIAA/ASME/ASCE/AHS 29th Structures, Structural Dynamics, and Materials Conference, Williamsburg, VA, April 18-20, 1988; received Oct. 24, 1988; revision received March 3, 1989.

*Senior Lecturer, Department of Civil Engineering.
†Professor, Faculty of Aerospace Engineering.

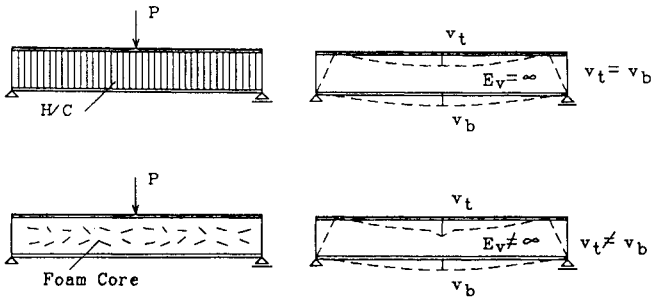

a) Geometry b) Deflections

Fig. 1 Deflections and geometry of a typical sandwich beam with and without vertical flexibility.

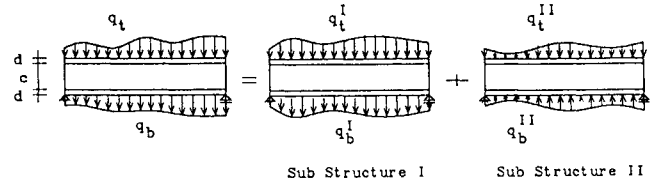

Fig. 2 Decomposition of a sandwich beam with soft core to two substructures.

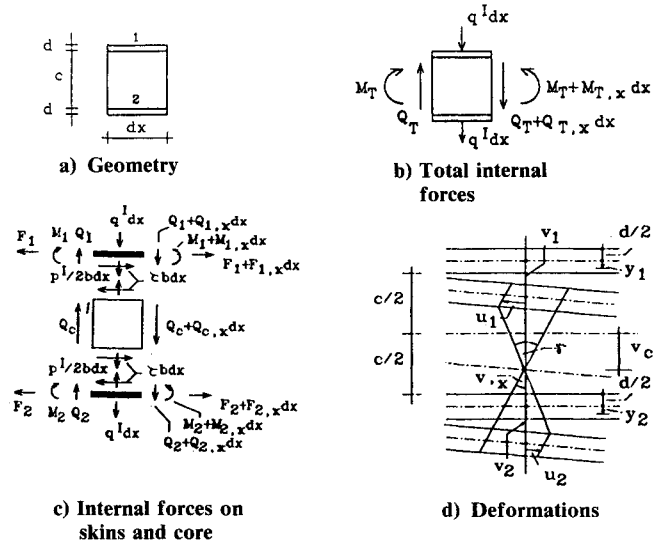

a) Geometry b) Total internal forces

c) Internal forces on skins and core d) Deformations

Fig. 3 Geometry, loads and internal resultants, and deformations of a differential segment (substructure I).

The shear stresses are uniform throughout the depth of the core since the normal stresses in the horizontal direction are negligible, thus,

$$\tau_{,x}c = -p^I \tag{4}$$

The deflection pattern is shown in Fig. 3d. Since the core height does not change during loading, the vertical displacements of the upper skin v_1, the lower skin v_2, and the core v_c are identical. The core contribution to the deformation pattern is due to its shear resistance only and is expressed by the shear angle γ. The kinematic relations between the horizontal displacement at the two skins and the vertical displacement and the shear strain are

$$u_1 = -(-v^I_{,x} + \gamma)c/2 + d/2v^I_{,x} - y_1 v^I_{,x} \tag{5a}$$

$$u_2 = (-v^I_{,x} + \gamma)c/2 + d/2v^I_{,x} - y_2 v^I_{,x} \tag{5b}$$

where v^I is the vertical deflection of the skin and the core, d the thickness of skin, and y_1 and y_2 are the vertical coordinates, measured from the center of gravity of the upper and lower skins, respectively. The shear strain is constant throughout the depth of the core and is equal to

$$\gamma = \tau/G_c \tag{6}$$

Substitution of Eq. (6) into Eqs. (5) yields

$$u_1 = -\frac{\tau c}{2G_c} + (c+d)\frac{v^I_{,x}}{2} - y_1 v^I_{,x} \tag{7a}$$

$$u_2 = \frac{\tau c}{2G_c} - (c+d)\frac{v^I_{,x}}{2} - y_2 v^I_{,x} \tag{7b}$$

By using the small-deflection theory assumptions and an equivalent modulus of elasticity for the skins, the internal forces take the form:

$$F_1 = (EA)_s\left[-\frac{\tau_{,x}c}{2G_c} + \frac{(c+d)}{2}v^I_{,xx}\right]$$

$$F_2 = -F_1$$

$$M_1 = -(EI)_s v^I_{,xx}, \qquad M_2 = M_1$$

$$(EA)_s = E_s bd, \qquad (EI)_s = E_s bd^3/12 \tag{8}$$

where $(EA)_s$ and $(EI)_s$ are the axial and the flexural rigidities of the skins, respectively; F_i and M_i $(i = 1,2)$ are the axial forces and the bending moments acting on each of the skins, respectively; and E_s is the equivalent modulus of elasticity of the skins.

The beam internal forces (Fig. 3a) are

$$Q_T = Q_1 + Q_2 + \tau cb \tag{9a}$$

$$M_T = M_1 + M_2 + F_2(c+d) \tag{9b}$$

Substitution of Eq. (8) into Eqs. (9), and after some mathematical operations, yields

$$M_{T,xx} = -2(EI)_s v^I_{,xxxx} + b\tau_{,x}(c+d) = -(q^I_t + q^I_b) \tag{10a}$$

$$F_{2,x} = (EA)_s[\tau_{,xx}c/2G_c - (c+d)v^I_{,xxx}/2] = \tau b \tag{10b}$$

After some algebraic manipulation, Eqs. (10) are replaced by

$$v^I_{,xxxx} - \tau_{,x}\delta = \frac{q^I}{(EI)_s} \tag{11a}$$

$$v^I_{,xxx} - \alpha\tau_{,xx} + \beta\tau = 0 \tag{11b}$$

where

$$\delta = \frac{(c+d)b}{2(EI)_s}, \qquad \alpha = \frac{c}{(c+d)G_c}, \qquad \beta = \frac{2b}{(c+d)(EA)_s} \tag{12}$$

The solution reads

$$v^I = C_1 + C_2 x + C_3 x^2 + C_4 x^3 + C_5 e^{sx} + C_6 e^{-sx} + v^I_p \tag{13a}$$

$$\tau = -6C_4/\beta + (s^3/\delta)\,C_5 e^{sx} - (s^3/\delta)\,C_6 e^{-sx} + \tau_p \tag{13b}$$

where $s = (\delta + \beta/\alpha)^{1/2}$ and v^I_p and τ_p are the particular solutions (solutions for other distributed loads appear in Appendix B). In the case of a uniformly distributed load, the particular

solutions reads

$$v_p^{\mathrm{I}} = \frac{\beta q^{\mathrm{I}}}{24(EI)_s(\delta+\beta)} x^4 \tag{14a}$$

$$\tau_p = -\frac{q^{\mathrm{I}}}{(EI)_s(\delta+\beta)} x \tag{14b}$$

The boundary conditions for a typical case at $x = 0,\ell$ (see Fig. 4) are

$$v^{\mathrm{I}} = 0 \tag{15a}$$

$$v^{\mathrm{I}}_{,xx} = 0 \tag{15b}$$

$$\tau^{\mathrm{I}}_{,x} = 0 \tag{15c}$$

which are equivalent to the conditions of a null axial force, bending moment, and vertical displacement. Other edge conditions appear in Appendix A. The continuity conditions at $x = x_1$ are

$$v^{\mathrm{I}(-)} = v^{\mathrm{I}(+)} \tag{16a}$$

$$v^{\mathrm{I}(-)}_{,x} = v^{\mathrm{I}(+)}_{,x} \tag{16b}$$

$$\gamma_c^{(-)} = \gamma_c^{(+)} \tag{16c}$$

$$F_2^{(-)} = F_2^{(+)} \tag{16d}$$

$$M_2^{(-)} = M_2^{(+)} \tag{16e}$$

$$Q_T^{(-)} - Q_T^{(+)} = 2P_e^{\mathrm{I}} \tag{16f}$$

where $(-)$ and $(+)$ refer to the sections to the left and right of the concentrated load, respectively. The condition in Eq. (16c) is because the deformations in the core are continuous at any point. In case of a beam with uniform properties, Eqs. (16) take the form:

$$v^{\mathrm{I}(-)} = v^{\mathrm{I}(+)} \tag{17a}$$

$$v^{\mathrm{I}(-)}_{,x} = v^{\mathrm{I}(+)}_{,x} \tag{17b}$$

$$\tau^{\mathrm{I}(-)} = \tau^{\mathrm{I}(+)} \tag{17c}$$

$$\tau^{\mathrm{I}(-)}_{,x} = \tau^{\mathrm{I}(+)}_{,x} \tag{17d}$$

$$v^{\mathrm{I}(-)}_{,xx} = v^{\mathrm{I}(+)}_{,xx} \tag{17e}$$

$$-(EI)_s[v^{\mathrm{I}(-)}_{,xxx} - v^{\mathrm{I}(+)}_{,xxx}] = P_e^{\mathrm{I}} \tag{17f}$$

In the case of a beam with nonuniform properties (see Fig. 4b), the continuity conditions are

$$v_1^{\mathrm{I}} = v_2^{\mathrm{I}} \tag{18a}$$

$$v^{\mathrm{I}}_{1,x} = v^{\mathrm{I}}_{2,x} \tag{18b}$$

$$\tau_1/G_1 = \tau_2/G_2 \tag{18c}$$

$$(EA)_{s_1}[\tau_{1,x}(c/2)G_1 - (c+d)v^{\mathrm{I}}_{1,xx}/2] = (EA)_{s_2}[\tau_{2,x}(c/2)G_2 - (c+d)v^{\mathrm{I}}_{2,xx}/2] \tag{19a}$$

$$(EI)_{s_1} v^{\mathrm{I}}_{1,xx} = (EI)_{s_2} v^{\mathrm{I}}_{2,xx} \tag{19b}$$

$$-2(EI)_{s_1} v^{\mathrm{I}}_{1,xxx} + \tau_1 b_1(c_1+d_1) + 2(EI)_{s_2} v_{2,xxx} - \tau_2 b_2(c_2+d_2) = 2P_e^{\mathrm{I}} \tag{19c}$$

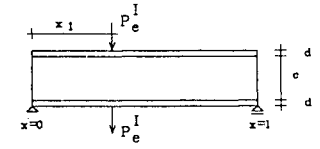

a) Uniform properties

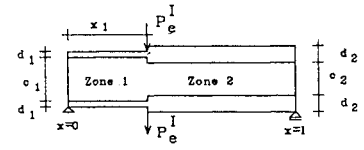

b) Nonuniform properties

Fig. 4 Typical sandwich beam with uniform and nonuniform properties loaded by a concentrated force.

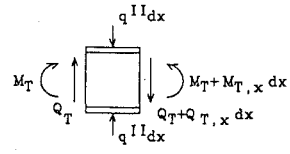

a) Loads and total internal forces

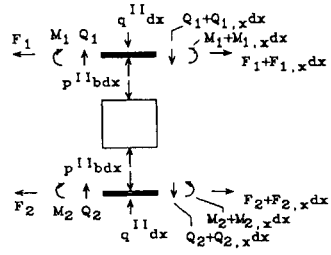

b) Internal forces on skins and core

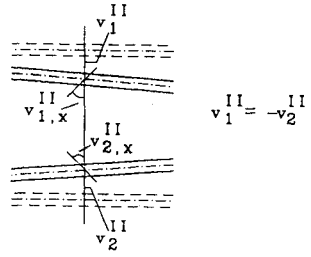

c) Deformations

Fig. 5 Loads, internal forces, and deformations of a differential segment (substructure II).

The condition in Eq. (18c) means that the shear stresses to the left and right of the joint are unequal. Thus, in addition to distributed transverse normal stresses, a concentrated force exists and equals

$$\tfrac{1}{2}(\tau_1 b_1 c_1 - \tau_2 b_2 c_2) = P_p^{\mathrm{I}} \tag{19d}$$

Substructure II

This substructure consists of two identical skins, a flexible core, and loaded by two self-equilibrated loads, $q_t^{\mathrm{II}} = q_b^{\mathrm{II}} =$

$(q_t - q_b)/2$. The internal forces at each skin and the core are self-equilibrated and the total shear and the bending moments are null. The core behavior remains elastic throughout the loading.

The equilibrium equations are derived by inspection of a differential element (see Fig. 5), and the deformations are symmetrical with respect to the centerline of the beam as shown in Fig. 5c. The upper and the lower skins displacements are the same but in opposite directions. Since core height is changed while its plane section remains vertical during the loading process, the shear stresses in the core as well as the horizontal normal forces in the skins are null.

Equilibrium equations for the various parts are as follows.

For the upper skin (plate 1):

$$Q_{1,x} = -q^{II} - p^{II}b \tag{20a}$$

$$M_{1,x} = Q_1 \tag{20b}$$

$$F_1 = 0 \tag{20c}$$

For the core:

$$Q_c = 0 \tag{21}$$

For the lower skin (plate 2):

$$Q_{2,x} = -q^{II} - p^{II}b \tag{22a}$$

$$M_{2,x} = Q_2 \tag{22b}$$

$$F_2 = 0 \tag{22c}$$

The change in the depth of the core is determined by modeling the core as made up of an infinite number of columns dx wide. These columns are loaded by the normal stresses at the interface, p^{II}.

The core remains elastic throughout the loading sequence, and the deformations throughout the depth are linear. The vertical deformation equals

$$v^{II} = \frac{p^{II}c}{2E_c} \tag{23}$$

where c is the height of the core and E_c is the vertical modulus of elasticity of the core. Using Eqs. (20) to (23), and $M_2 = -(EI)_s v_{,xx}$ yields

$$(EI)_s v^{II}_{,xxxx} + \frac{2bE_c}{c} v^{II} = q^{II} \tag{24}$$

Equation (24) may be considered as that of a beam resting on an elastic foundation,[12] with a spring coefficient equal to

$$k_c = \frac{2E_c b}{c} \tag{25}$$

Thus, substructure II is modeled as two beams (skins) resting on an elastic foundation, which is provided by the flexibility of the core.

The general solution of Eq. (24) takes the form:

$$v^{II} = C_1 \cos\lambda x \cosh\lambda x + C_2 \sin\lambda x \cosh\lambda x + C_3 \cos\lambda x \sinh\lambda x + C_4 \sin\lambda x \sinh\lambda x + v_p^{II} \tag{26}$$

where

$$\lambda = \left[\frac{bE_c}{2c(EI)_s}\right]^{1/4} \quad \text{and} \quad v_p^{II} = \frac{q^{II}c}{2bE_c}$$

for a uniformly distributed load. (Additional solutions for other distributed loads appear in Appendix B.)

The deflections and the internal stresses are determined by the solution in Eq. (26) with the appropriate boundary conditions. The boundary conditions are demonstrated for the example shown in Fig. 4 and equal to the following.

At $x = 0, \ell$:

$$v^{II} = 0 \tag{27a}$$

$$(EI)_s v^{II}_{,xx} = 0 \tag{27b}$$

At $x = x_1$:

$$v^{II(-)} = v^{II(+)} \tag{28a}$$

$$v^{II(-)}_{,x} = v^{II(+)}_{,x} \tag{28b}$$

$$(EI)_s v^{II(-)}_{,xx} = (EI)_s v^{II(+)}_{,xx} \tag{28c}$$

$$-(EI)_s v^{II(-)}_{,xxx} + (EI)_s v^{II(+)}_{,xxx} = P_e^{II} \tag{28d}$$

The solutions for other cases can be found in Ref. 12.

General Behavior

The general behavior of the sandwich beam is expressed by the superposition of the two substructure behaviors discussed previously. The deformations, shear forces, and bending moments in the two skins are a combination of the two substructures. The axial forces at the skins and the shear stresses at the interface and the core are solely due to the response of the first substructure. The transverse normal stresses at the interfaces are affected by the behavior of the two substructures.

Numerical Analysis

A computer code based on the principles outlined in the preceding sections was developed. The code allows any combination of loadings, boundary conditions, and any continuity conditions, such as extensional or rotational springs. The beam considered may be nonuniform piecewise, i.e., its geometry and mechanical properties differ from one part to another, but remain uniform within the region. It is recommended to use the conditions of symmetry wherever possible, since the analytical solution consists of hyperbolic functions which tend to grow very quickly as their arguments reach values of 150 and above. The code is used for a parametric study of some typical sandwich beams.

The main parameters considered are 1) type of load (uniform, concentrated); 2) properties of core (geometrical and mechanical); 3) skin properties (thickness and modulus of elasticity); and 4) boundary conditions.

The parametric study inlcudes two types of beams, as shown in Figs. 6 and 10.

The first example deals with a beam simply supported at the edges and loaded at midspan, as shown in Fig. 6a. The skins are laminated composite with $E_{\text{eff}} = 2742$ kg/mm^2 and $G = 160$ kg/mm^2 and the foam core with $E_c = 5.25$ kg/mm^2 and $G_c = 2.1$ kg/mm^2. The concentrated load is transferred to the beam with the aid of a metal tab 20-mm wide and 60-mm long. The effects of the load distribution under the tabs (see Fig. 7) on the performance of the beam is investigated; see Figs. 6 and 8.

The following conclusions can be drawn from the results:

1) The flexibility of the core yields local effects in general.

2) The deflections of the loaded skin (upper) are larger than the lower one in the vicinity of the loaded area and become identical far from the loaded zone; see Fig. 6b.

3) The axial force distribution follows the bending-moment diagram of a beam loaded by a concentrated load at midspan; see Fig. 6c.

4) The shear stresses are nonuniform in the vicinity of the

loaded area and uniform along the rest of the beam. Shear stresses in the core at midspan are null even in the case of a concentrated load, due to the symmetry and the continuity requirements. The exact stress distribution in the loaded zone depends on the loading distribution function.

5) Stresses in the adhesive layers, between the skins and the core, in the vicinity of the loaded area appear in Fig. 8. It is compressive in the upper interface and tensile in the lower one. The effect of the distribution of the load is demonstrated through five types of load distributions with a resultant of 50 kg (see Fig. 7). The contact stress distribution under the loaded tab depends on the flexural-rigidity ratio of the tab and the beam underneath. In the case of a very flexible tab, the contact stress distribution resembles that of a concentrated load, denoted by OF, while at the other extreme, a very stiff tab, it changes to two concentrated loads pattern, denoted by TF; see Fig. 7. Intermediate ratios of rigidities lead to the distributions denoted by SIN, UNIF, and CONSIN, as described in Fig. 7. The exact contact stress distribution demands a thorough analysis which is beyond the scope of this research. The extreme normal transverse stresses occur when the tab is very flexible (see the OF curve). Under a very stiff tab (see TF curve), the largest value is reduced to a half of the maximum under the flexible tab and becomes a quarter of that value for the intermediate tab rigidities; see UNIF, SIN, and CONSIN curves. The stresses at the lower interface are small

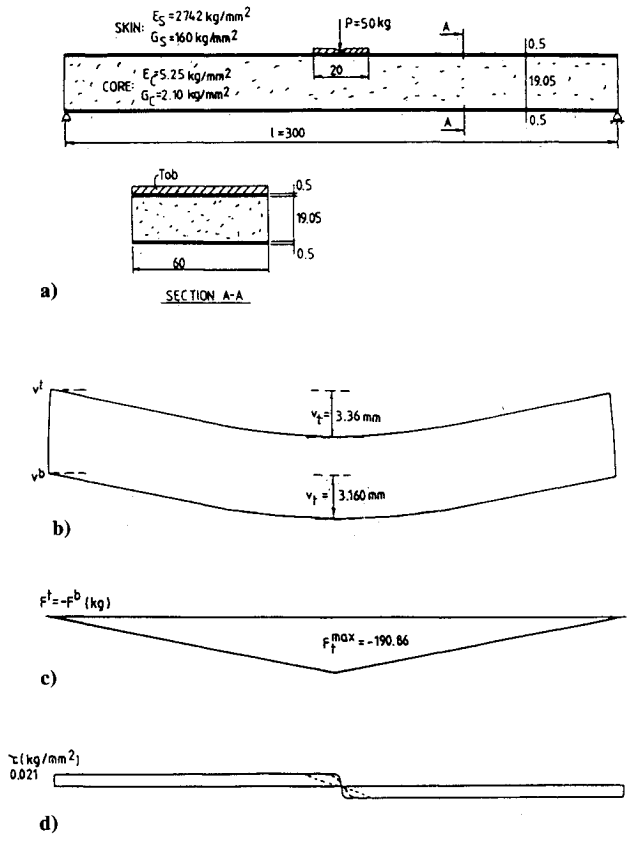

Fig. 6 Three-point bending results: a) loads, geometry, and mechanical properties; b) deflections; and c) axial resultants at upper and lower skins and shear stresses at adhesive layer.

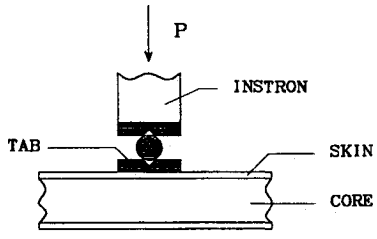

a) Load configuration

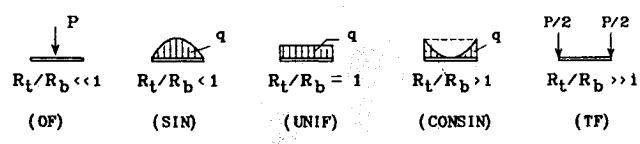

b) Contact stress distributions

Fig. 7 Load configuration and contact stress distributions under the loaded tab for various rigidity ratios (R_t = tab flexure rigidity; R_b = beam flexure rigidity under tab).

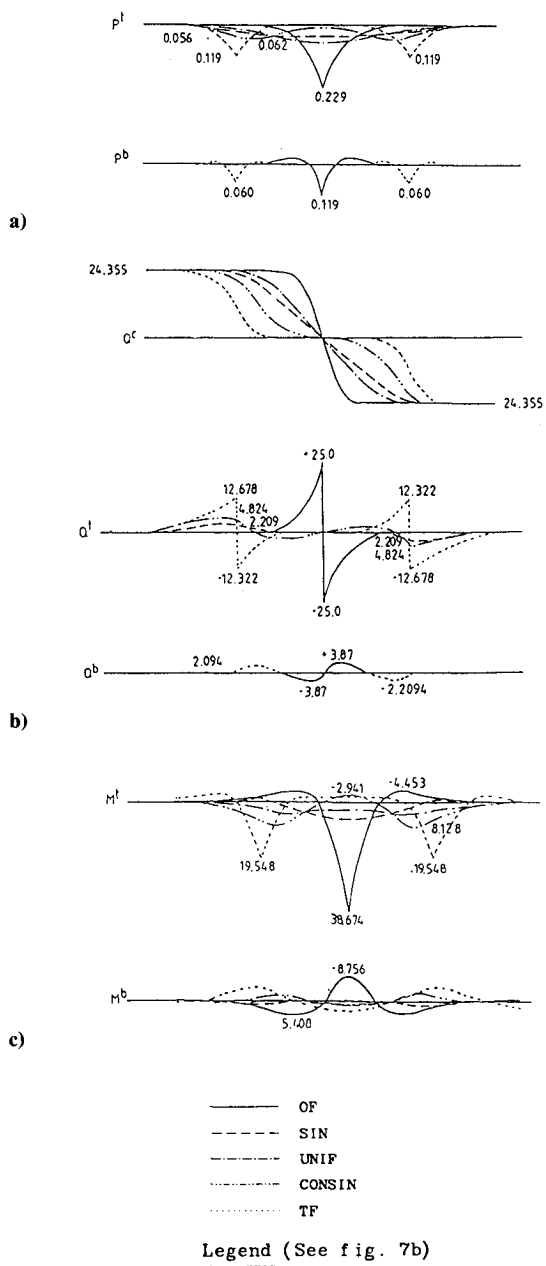

Fig. 8 Internal stress distributions in the vicinity of the loaded zone for the three-point bending beam: a) normal stresses in adhesive layers; b) shear forces in the skins and the core; and c) bending moments in the skins.

compared to that of the upper one and are only significant in the case of a stiff tab, and negligible in other cases.

6) Shear force distribution in the vicinity of the load appear in Fig. 8b. The shear forces in the skins are significant at the loaded zone, but become null far from the loaded area. In the core, the forces become null at midspan due to symmetry and continuity requirements of the deflection function. Thus, in the vicinity of the loaded area, the shear forces are actually transferred from the core to the skin leading to large forces in the case of very flexible or very stiff tabs and negligible under intermediate tab-rigidities ratio. In the case of a very flexible tab, using the concentrated load distributions (see Fig. 7), the shear at midspan is resisted by the skins only (see Fig. 8b), while to the left and right of that location the skins and the core participate in resisting the shear forces. In the other case with the very stiff tab, using the two concentrated loads distribution (see Fig. 7), the zone in between the two concentrated loads is subjected to self-equilibrated shear forces. Here the shear forces in the skins are counteracted by the forces in the core, and usually reach their extreme values at the end of this zone (see Fib. 8b). The shear forces at the lower skin are small compared to the upper one.

7) The bending moments in the skins are a measure of the curvatures and bending stresses induced in the two skins. The bending moments are large in the case of a very flexible or very stiff tab and are moderate under other tab rigidities.

8) The flexibility of the core leads to local effects, which under some load distributions become very significant and can even cause a sudden collapse of the structure.

The second example demonstrates the effect of a cantilever on the overall behavior of the structure; see Fig. 9. Its effect is local, limited to the vicinity of the support, and the behavior in the other regions is unaffected. The deflections of the cantilever part are nonlinear and consist of a small curvature left of the support, as opposed to the ordinary theory of beams, even though the cantilever is not loaded externally. The internal forces and stresses are distributed to the left and right of the support; see Fig. 9. The transverse tensile normal stresses at the upper skin are shown in Fig. 9b. The shear force distribution left of the support is self-equilibrated and the forces in the skins are counteracted by the forces acting on the core; see Fig. 9d. The bending moments in the skins are in equilibrium with the small axial forces induced in the upper and lower skins, thus leading to curvatures in the cantilever region. The major conclusion from this example is that the cantilever parts of a sandwich beam with transversely flexible core are experiencing stresses in the vicinity of the support and nonlinear deformation pattern throughout the cantilever length.

The third example deals with a beam, loaded at two points, 75-mm apart, symmetric, and simply supported. The geometry and the mechanical properties appear in Fig. 10a. Results, presented in Fig. 10, include deflections, internal shear forces, and transverse normal stresses at the interface layers in the vicinity of the loaded zone. The beam is loaded by two concentrated loads, 50 kg each at $x = \ell/4$ and $3/4\ell$. The loads are transferred to the beam with two tabs, 20-mm wide. The

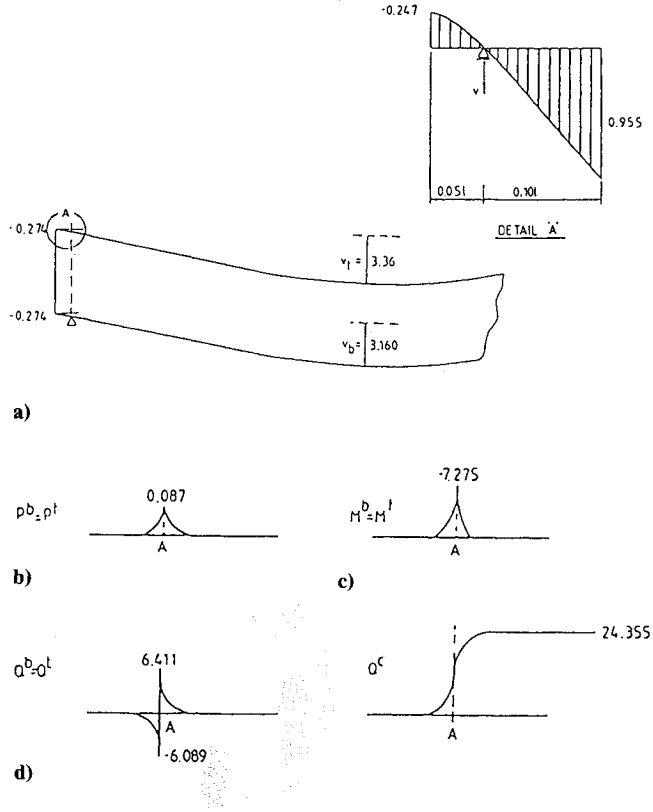

Fig. 9 Results for a cantilevered three-point beam in the vicinity of the support: a) deflections; b) normal stresses in adhesive layers; c) bending moments at the skins; and d) shear forces at the skins and the core.

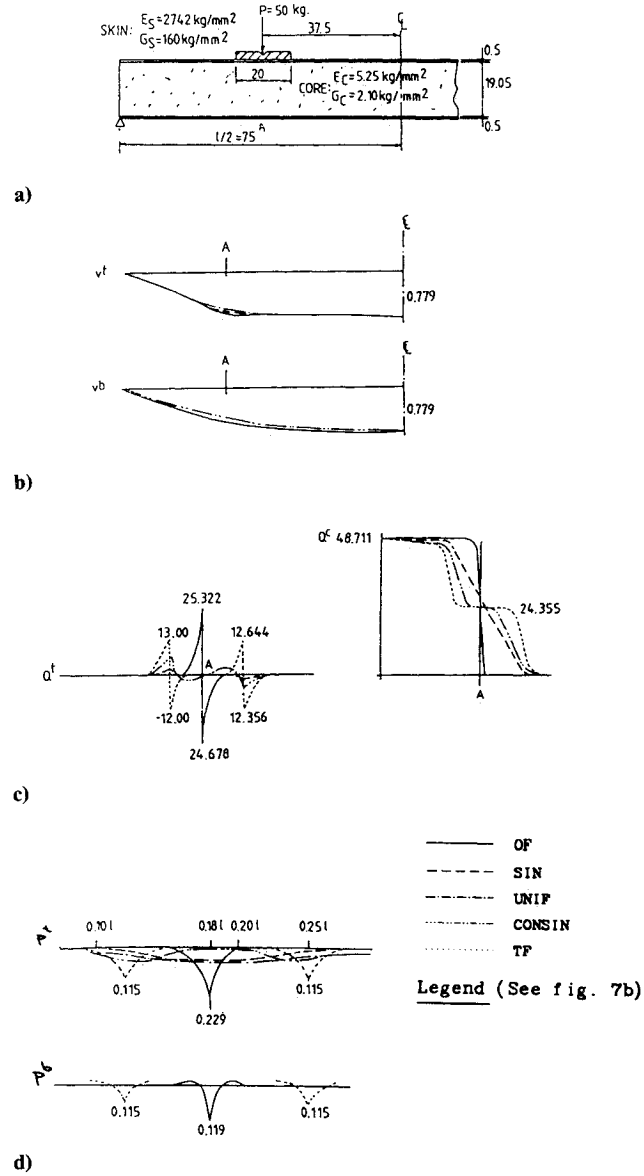

Fig. 10 Four-point bending beam results: a) load, geometry, and mechanical properties; b) skins deflections; c) shear forces in the skins and the core; and d) normal stresses at upper and lower interfaces.

loading pattern exerted on the beams follows the distributions described in Fig. 7.

The following conclusions may be drawn from the results:

1) The overall deflection pattern of the beam is independent of the exact contact stress distribution under the tab (concentrated or distributed). The differences are in the vicinity of the loaded zone only. The deflection at midspan is the same for all types of loading (Fig. 10b).

2) Shear forces in the core and in the upper skin appear in Fig. 10c. Here, contrary to the case described in the first example (see Fig. 8b), the shear forces in core, under a very flexible tab, denoted by the OF curve, are not null. These forces reach their maximum in case of a very flexible tab. In all of the loading cases, the core and the skin participate in the shear resistance and each one carries half of the magnitude of the external load in the region left of the loaded zone. In the region right of that zone, the shear forces in the core are counteracted by the shear forces in the skins.

3) The normal stresses at the upper and the lower interfaces appear in Fig. 10d. The maximum is reached when the tab is very flexible and is reduced to about a quarter of that value in the case of a very stiff tab.

The last example, see Fig. 11, compares the results of the proposed method, for a sandwich beam loaded by a concentrated load at midspan, with finite-element analysis; see Ref. 13. The deflections in the upper skin are nearly identical, about 0.5% difference, and at the lower skin, they differ by about 2.5% at the most. The internal forces are identical far from the loaded zone but differ in load vicinity. The differences are due to the singularity near the concentrated force which is actually "smeared" by the finite-element code.

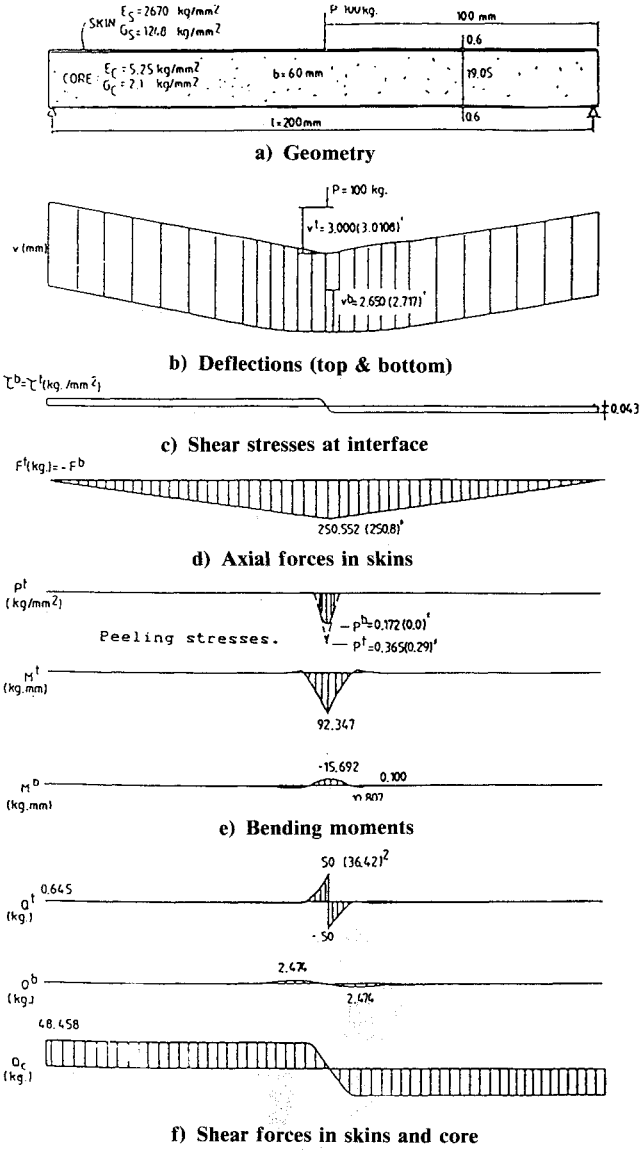

Fig. 11 Results comparisons with NASTRAN (finite elements) using a three-point bending beam (finite-element results in parentheses).

Conclusions

The general behavior of a sandwich beam with flexible core, loaded by concentrated loads and distributed loads, is analyzed. The bending behavior is modeled by superposition of two types of beam behavior. The first one, substructure I, consists of a core with shear rigidity only. The second one, substructure II, allows the core to be flexible in the vertical direction. It enables the effects of localized loads to be included in the analysis. The shear stresses and axial forces in the skins are only due to the core rigidity of the first substructure. The transverse normal stresses, at the skin-core interface layers, and the other internal forces in the skins are affected by the behavior of the two substructures. The contributions to the internal forces from each substructure depends on the geometrical and mechanical properties as well as the ratio of the length to the depth of the beam.

The effect of the elastic foundation, substructure II, on the general behavior becomes significant as the ratio of length to depth is reduced.

The proposed analysis can determine, by the use of simple beam theory, the transverse normal stresses at the interface layers between the skin and the core in the vicinity of concentrated loads. In some cases these stresses are significant, compared with the allowable stresses of the core material, and may cause a sudden failure of the structure.

In the case of beams loaded through tabs or by other localized loads, the behavior in the loaded region is significantly affected by the shape of the load distribution. In the unloaded regions, the behavior is only affected by the resultants of the localized loads. The internal forces and stresses involved are significant in cases of very flexible or very stiff tabs.

The proposed analysis enhances the physical insight of the beam behavior, especially under localized loads and gives some explanations concerning the transverse and shear stresses between the skin face and the core. The stresses involved become significant under localized loads, and their magnitude might be crucial to the safety of the structure. In such cases, the use of the proposed analysis is more than recommended.

Appendix A: Boundary Conditions for Substructure I

The continuity and boundary conditions are described below, and description of the edge conditions follows.

Edge Joints

1) Simply supported:

$$v = 0 \tag{A1a}$$

$$v_{,xx} = 0 \tag{A1b}$$

$$\tau_{,x} = 0 \tag{A1c}$$

2) Clamped:

a) Immovable at the skins (the two skins cannot slide horizontally): $u_{skin} = 0$

$$v = 0 \tag{A2a}$$

$$v_{,x} = 0 \tag{A2b}$$

$$\tau = 0 \tag{A2c}$$

b) Movable at the skins (one of the skins can slide horizontally with respect to the other one): $u_{\text{skin}} \neq 0$

$$v = 0 \tag{A3a}$$

$$v_{,x} = 0 \tag{A3b}$$

$$\tau_{,x}c_1/2G_{c_1} - (c_1 + d_1)v_{,xx}/2 = 0 \tag{A3c}$$

3) Sliding fixity:

a) Immovable at the skins: $u_{\text{skin}} = 0$ (the two skins cannot slide horizontally). Equations (A4) describe the condition at the symmetry axis

$$v_{,x} = 0 \tag{A4a}$$

$$\tau = 0 \tag{A4b}$$

$$v_{,xxx} = 0 \tag{A4c}$$

b) Movable at the skins: $u_{\text{skin}} \neq 0$ (one of the skins can slide horizontally with respect to the other one).

$$v_{,x} = 0 \tag{A5a}$$

$$\tau_{,x}c_1/2G_{c_1} - (c_1 + d_1)v_{,xx}/2 = 0 \tag{A5b}$$

$$-2(EI)_{s_1}v_{,xxx} + \tau b_1(c_1 + d_1) = 0 \tag{A5c}$$

4) Free:

$$v_{,xx} = 0 \tag{A6a}$$

$$\tau_{,xx} = 0 \tag{A6b}$$

$$-2(EI)_{s_1}v_{,xxx} + \tau b_1(c_1 + d_1) = 0 \tag{A6c}$$

Inner Joints (Between Segments $i-1$ and i)

1) Continuous over a support:

$$v_{i-1} = 0 \tag{A7a}$$

$$v_i = 0 \tag{A7b}$$

$$v_{i-1,x} = v_{i,x} \tag{A7c}$$

$$\tau_{i-1}/G_{i-1} = \tau_i/G_i \tag{A7d}$$

$$(EA)_{s_{i-1}}[\tau_{i-1}c_{i-1}/2G_{c_{i-1}} - (c_{i-1} + d_{i-1})v_{i-1,xx}/2]$$
$$= (EA)_{s_i}[\tau_i c_i/2G_{c_i} - (c_i + d_i)v_{i,xx}/2] \tag{A7e}$$

$$(EI)_{s_{i-1}}v_{i-1,xx} = (EI)_{s_i}v_{i,xx} \tag{A7f}$$

2) Continuous over a flexible support (translation spring, k_v):

$$v_{i-1} = 0 \tag{A8a}$$

$$v_{i-1,x} = v_{i,x} \tag{A8b}$$

$$\tau_{i-1}/G_{c_{i-1}} = \tau_i/G_{c_i} \tag{A8c}$$

$$(EA)_{s_{i-1}}[\tau_{i-1}c_{i-1}/2G_{c_{i-1}} - (c_{i-1} + d_{i-1})v_{i-1,xx}/2]$$
$$(EA)_{s_i}[\tau_i c_i/2G_{c_i} - (c_i + d_i)v_{i,xx}/2] \tag{A8d}$$

$$(EI)_{s_{i-1}}v_{i-1,xx} = (EI)_{s_i}v_{i,xx} \tag{A8e}$$

$$-2(EI)_{s_1}v_{,xxx} + \tau_i(c_{i-1} + d_{i-1})b_i + 2(EI)_{s_{i-1}}v_{,xxx}$$
$$-\tau_i(c_i + d_i)b_i = k_v v_{i-1} \tag{A8f}$$

Appendix B: Particular Solution for Various Distributed Loads

Particular Solutions for Substructure I

1) $q^{\text{I}} = q_o \sin\pi x/a$:

$$v_P \frac{[q_o/(EI)_s]\ [\alpha(\pi/a)^2 + \beta]}{(\pi/a)^4[\alpha(\pi/a)^2 + \beta + \delta]} \sin\frac{\pi x}{a} \tag{B1a}$$

$$\tau_P = \frac{q_o}{(EI)_s}\left(\frac{a}{\pi}\right)\frac{1}{[\alpha(\pi/a)^2 + \beta + \delta]}\cos\frac{\pi x}{a} \tag{B1b}$$

2) $q^{\text{I}} = q_o\,(x/a)$:

$$v_P = \frac{q_o}{120a(EI)_s(\delta + \beta)}(-\beta x^5 - 20\alpha x^3) \tag{B2a}$$

$$\tau_P = -\frac{q_o}{2a(EI)_s(\delta + \beta)}x^2 \tag{B2b}$$

3) $q^{\text{I}} = q_o\,(1 - x/a)$:

$$v_P = \frac{q_o}{(EI)_s(\delta + \beta)}\left[\frac{\beta x^4}{24} + \frac{1}{120}(\beta x^5 + 20\alpha x^3)\right] \tag{B3a}$$

$$\tau_P = -\frac{q_o}{(EI)_s(\delta + \beta)}\left(x - \frac{x^2}{2a}\right) \tag{B3b}$$

4) $q^{\text{I}} = q_1 - q_2 \sin(\pi x/a)$:

$$v_P = \frac{1}{(EI)_2}\left[\frac{\beta x^4}{24(\delta + \beta)}q_1 - \frac{[\alpha(\pi/a)^2 + \beta]}{(\pi/a)^4[a(\pi/a)^2 + \beta + \delta]}q_2\right] \tag{B4a}$$

$$\tau_P = \frac{1}{(EI)_2}\left[-\frac{x}{(\delta + \beta)}q_1 - \frac{1}{(\pi/a)[\alpha(\pi/a)^2 + \beta + \delta]}q_2\right] \tag{B4b}$$

Particular Solutions for Substructure II

1) $q^{\text{II}} = q_o \sin\pi x/a$:

$$v_P = \frac{q_o}{\left[(EI)_s(\pi/a)^4 + \dfrac{2bE_c}{c}\right]}\sin\frac{\pi x}{a} \tag{B5}$$

2) $q^{\text{II}} = q_o x/a$:

$$v_P = \frac{q_o c}{2baE_c}x \tag{B6}$$

3) $q^{\text{II}} = q_o\,(1 - x/a)$:

$$v_P = \frac{q_o c}{2baE_c}(1 - x/a) \tag{B7}$$

4) $q^{\text{II}} = q_1 - q_2 \sin(\pi x/a)$:

$$v_P = \frac{q_1 c}{2bE_c} - \frac{q_2}{\left[(EI)_s(\pi/a)^4 + \dfrac{2bE_c}{c}\right]}\sin\frac{\pi x}{a} \tag{B8}$$

References

[1]Reissner, E., "On Bending of Elastic Plates," *Quarterly Journal of Applied Mathematics*, Vol. 5, April 1947, pp. 55–68.

[2]Reissner, E., "Finite Deflections of Sandwich Plates," *Journal of the Aeronautical Sciences*, Vol. 15, July 1948, pp. 435–440.

[3]Hockman, L. E., "Sandwich Construction and Design," *Analysis and Design of Flight Vehicle Structure*, edited by E. F. Bruhn, S. R. Jacobs & Associates, IN, 1973, Chap. 12.

[4]Schwartz, R. T. and Rosato, D. V., "Structural-Sandwich Construction," *Composite Engineering Laminates,* edited by A. G. H. Dietz, MIT Press, Cambridge, MA, 1969, pp. 165-194.

[5]Allen, H. G., *Analysis and Design of Structure Sandwich Panels,* Pergamon, Oxford, London, 1969, Chap. 2.

[6]*Mechanical Properties of Hexcel Honeycomb Materials,* TSB120, Hexcel Corp., Dubin, CA, 1982.

[7]Holt, D. J. and Webber, J. P. H., "Exact Solution to Some Honeycomb Sandwich Beam, Plate, and Shell Problems," *Journal of Strain Analysis,* Vol. 17, No. 1, 1982, pp. 1-8.

[8]Pearce, T. R. A., "The Stability of Simply Supported Sandwich Panels with Fiber-Reinforced Faceplates," Ph.D. Thesis, Univ. of Bristol, UK, Sept. 1973.

[9]Monforton, G. R. and Ibrahim, I. M., "Modified Stiffness Formulation of Unbalanced Anisotropic Sandwich Plates," *International Journal of Mechanical Sciences,* Vol. 19, June 1977, pp. 335-343.

[10]Ojalvo, I. V., "Departures from Classical Beam Theory in Laminated Sandwich and Short Beams," *AIAA Journal,* Vol. 15, Oct. 1977, pp. 1518-1521.

[11]Ogorkiewicz, R. M. and Sayigh, A. A. M., "Deflection of Carbon Fiber/Acrylic Foam Sandwich Beams," *Composites,* Vol. 4, Nov. 1973, pp. 254-257.

[12]Hetenyi, M., *Beams on Elastic Foundation,* The University of Michigan Press, Ann Arbor, MI, 1958, Chap. 1-5.

[13]MacNeal, R. H., *MSC/NASTRAN Application Manual, V.65,* MacNeal-Schwendler Corp., Los Angeles, CA, 1972.